Target Identification

DOI: 10.1002/anie.201310618

Phenotypic Screening to Identify Small-Molecule Enhancers for Glucose Uptake: Target Identification and Rational Optimization of Their Efficacy**

*Minseob Koh, Jongmin Park, Ja Young Koo, Donghyun Lim, Mi Young Cha, Ala Jo, Jang Hyun Choi, and Seung Bum Park**

Abstract: *Small-molecule glucose uptake enhancers targeted to myotubes and adipocytes were developed through a phenotypic screening linked with target identification and rational optimization. The target protein of glucose-uptake enhancers was identified as a nuclear receptor PPARγ (peroxisome proliferator-activated receptor gamma). Subsequent optimization of initial hits generated lead compounds with high potency for PPARγ transactivation and cellular glucose uptake. Finally, we confirmed that the chirality of optimized ligands differentiates their PPARγ transcriptional activity, binding affinity, and inhibitory activity toward Cdk5 (cyclin-dependent kinase 5)-mediated phosphorylation of PPARγ at Ser273. Using phenotype-based lead discovery along with early-stage target identification, this study has identified a new small-molecule enhancer of glucose uptake that targets PPARγ.*

Owing to the increasing morbidity associated with type 2 diabetes involving microvascular complications, the identification of effective methods to control hyperglycemia is considered a top priority in the biomedical community.[1] Normal glucose levels can be maintained by regulating insulin sensitivity in skeletal muscles, glycogenolysis in the liver, and lipolysis in fat tissue.[2] Therefore, the development of novel small molecules that regulate cellular glucose uptake or insulin sensitivity in muscles or fat tissues would provide promising candidates to treat type 2 diabetes and related complications.

To facilitate the discovery of novel anti-diabetic agents, we envisioned the conjunction of target identification with phenotypic screening: 1) Image-based high-throughput screening (HTS)[3] using a fluorescent glucose analogue, GB2, to identify small-molecule modulators of glucose uptake in myotubes;[4] 2) identification of the target protein of initial hits from a phenotypic assay by FITGE (fluorescence difference in two-dimensional gel electrophoresis) technology;[5] and 3) rational hit-to-lead optimization.

First, we performed the image-based HTS of a 3000-membered drug-like compound library derived from a privileged substructure-based diversity-oriented synthesis strategy[6] in a 96-well plate format. Fluorescence intensity of GB2 in the cytoplasm of the differentiated C2C12 myotubes was quantified from captured images in an automated fashion, which identified small-molecule enhancers of cellular glucose uptake. Among the initial hit compounds, we were particularly interested in two isoxazole-containing compounds (P29C06 and P29C07) because they selectively enhanced cellular glucose uptake in C2C12 myotubes, but not in undifferentiated C2C12 myoblasts. Their different glucose uptake capabilities related to the differentiation status of C2C12 cells were quantitatively investigated in myoblasts and myotubes by direct comparison with ampkinone, a small-molecule glucose uptake enhancer that functions by the induction of AMP-activated protein kinase phosphorylation (Figure 1a; Supporting Information, Figure S1a,b).[7] This phenotypic observation suggested that the cell differentiation-dependent enhancement of cellular glucose uptake may be caused by the elevated quantity of target proteins in myotubes compared to the pre-differentiated counterparts. Given the fact that both P29C06 and P29C07 also enhanced cellular glucose uptake in adipocytes, our initial hit compounds were considered to affect energy homeostasis.[8]

After identifying the initial hits from the phenotypic screening, we pursued the target identification of glucose uptake enhancers using FITGE technology, a fluorescence-guided target identification method involving a photoaffinity probe.[5] Preliminary structure–activity relationship studies led us to modify P29C06 to generate a probe (P29C06-Az) for FITGE. As shown in Figure 1c, P29C06-Az contains aryl azide as a photoaffinity group and an acetylene moiety as a bioorthogonal handle for the visualization of cross-linked proteomes using a fluorescence reporter.[9] Despite structural changes, the probe retained its bioactivity in the myotubes

[*] Dr. M. Koh, Dr. J. Park, J. Y. Koo, Dr. M. Y. Cha, A. Jo, Prof. Dr. S. B. Park
Department of Chemistry, Seoul National University
Seoul 151-747 (Korea)
E-mail: sbpark@snu.ac.kr
D. Lim, Prof. Dr. S. B. Park
Department of Biophysics and Chemical Biology
Seoul National University
Seoul 151-747 (Korea)
Prof. Dr. J. H. Choi
School of Nano-Bioscience & Chemical Engineering
Ulsan National Institute of Science and Technology
Ulsan 689-798 (Korea)

[**] This work was supported by the Global Frontier Project Grant (2013M3A6A4044245), the Bio & Medical Technology Development Program (2012M3A9C4048780), the Basic Research Laboratory (2010-0019766), and Basic Science Research Program (2012R1A1A1015407) funded by the National Research Foundation of Korea (NRF). M.K., J.P., J.Y.K., D.L., and A.J. are grateful for a BK21 Scholarship.

Supporting information for this article is available on the WWW under http://dx.doi.org/10.1002/anie.201310618.

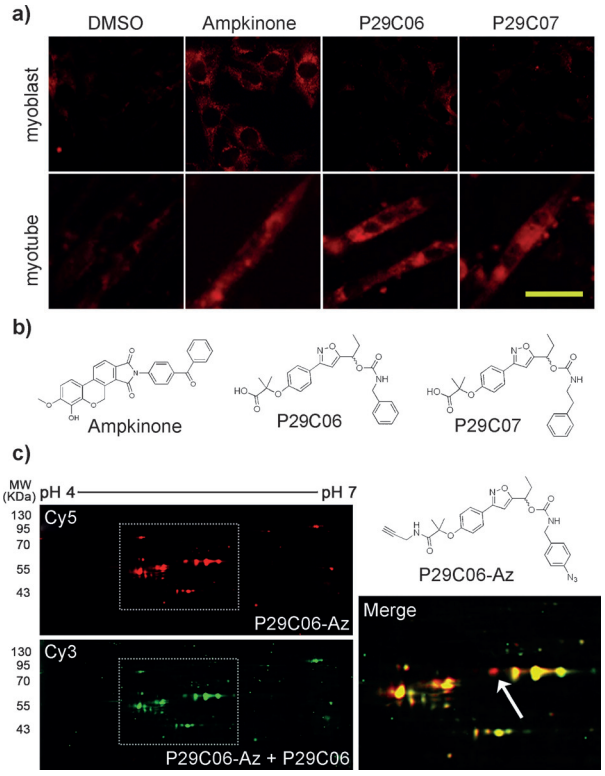

Figure 1. Target identification of small-molecule glucose uptake enhancers. a) Fluorescence microscopic images of C2C12 myoblasts and myotubes 24 h after treatment with each compound using the GB2 procedure. Scale bar: 10 μm. b) Chemical structures of ampkinone, P29C06, and P29C07. c) FITGE-based target identification of P29C06 using photoaffinity probe, P29C06-Az. Two-dimensional gel images were acquired in the Cy3 or Cy5 channel using a fluorescence scanner. The merged image shows the target protein selectively labeled in red (white arrow).

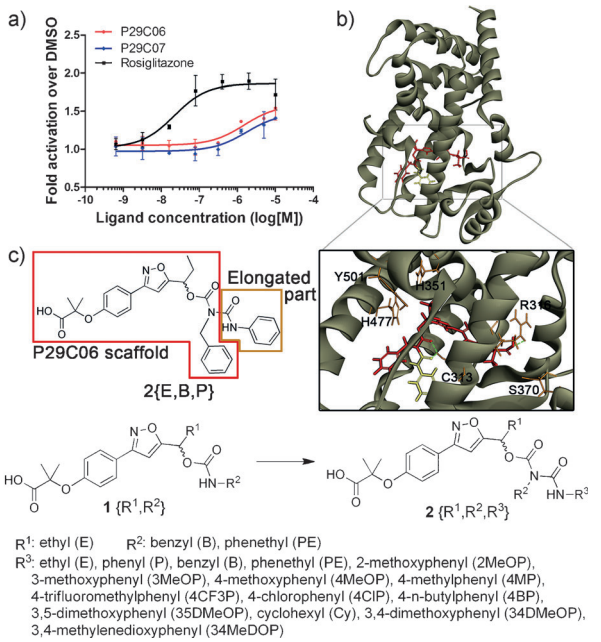

Figure 2. Target validation and structural optimization of primary hit compounds. a) Transactivation profiles of rosiglitazone, P29C06, and P29C07 using a PPARγ-derived reporter gene in 293T cells at 24 h after treatment ($n=3$). Error bars, s.d. b) Docking analysis of **2**{E,B,P} using crystal structure of PPARγ ligand-binding domain (LBD) (PDB ID: 2hfp; Discovery Studio 1.7 [Accelrys] was used; Cys313 was intentionally tilted for better fit; hydrogen bonding is illustrated by the light green dashed line). c) Design of optimized leads. Detailed synthetic procedure is described in Supporting Information.

and adipocytes (Supporting Information, Figure S1c,d). To induce covalent tethering of P29C06-Az to its target proteins, the probe was incubated with live myotubes for 3 h, followed by UV irradiation for 30 min. The cells were then lysed and treated with an azide-containing Cy5 reporter to visualize P29C06-Az-protein complexes by click chemistry. To eliminate false-positive signals owing to non-specific labeling with photoaffinity probe, an excess of soluble competitor (P29C06) was added as a negative control in an identical procedure, where the Cy3 reporter was used for bioorthogonal labeling. The following experiments and analysis were performed as previously described.[5] Unfortunately, we were unable to identify target protein candidates in C2C12 myotubes, which might be due to the low expression levels of target proteins. On the other hand, we successfully identified a number of potential target proteins by mass analysis in differentiated 3T3L1 adipocytes (Figure 1c; Supporting Information, Figures S2, S3, Tables S1, S2). Among them, we identified PPARγ as the target protein. In fact, PPARγ is a member of the nuclear receptor family and has been shown to play important roles in energy homeostasis and glucose metabolism[10] associated with insulin sensitization and adipogenesis. Furthermore, its agonistic ligand, rosiglitazone, has been used as an oral therapeutic for the treatment of type 2 diabetes.[11]

For the validation of the outcome of FITGE-based target identification, we subjected the initial hits to a cell-based PPARγ-luciferase transactivation assay. As shown in Figure 2a, P29C06 and P29C07 exhibited partial agonism toward PPARγ with moderate efficacy (EC_{50}: 1.5 and 1.7 μM, respectively). The differential pattern of cellular glucose uptake in myotubes and myoblasts upon treatment with hit compounds might be due to the expression level of PPARγ (Supporting Information, Figure S4). Moderate activity of the initial hits drove us to pursue a rational drug discovery approach with the structural and functional information of PPARγ. Based on the docking simulation, the initial hit compound P29C06 occupies the ligand-binding site[12] of PPARγ with some extra space that can be utilized to enhance its efficacy as well as selectivity (Figure 2b; Supporting Information, Figure S5). Therefore, we designed and synthesized a series of analogues to improve their efficacy in cellular glucose uptake (Figure 2c). First, we confirmed that the direct analogues of initial hits, **1**{R^1,R^2}, having ethyl (E) group at the R^1 position and either benzyl (B) or phenethyl (PE) group at the R^2 position showed better transcriptional activity of PPARγ (Supporting Information, Figure S6). Next, we decorated **1**{E,B} and **1**{E,PE} with a second set of isocyanates to generate a 1,3-dicarbonyl moiety, which was predicted to be more tightly bound at the ligand-binding site of PPARγ via an additional hydrogen bonding with Cys313 (Figure 2b). To confirm the selectivity as well as the efficacy, we examined the resulting series of analogues in cell-based transactivation

Table 1: Transactivation profiles of WY14643, GW501516, rosiglitazone, and compounds **1** and **2** using a PPAR-derived reporter gene in 293T cells at 24 h after treatment with each compound.[a]

Entry	Compounds	PPARα	PPARδ	PPARγ
1	**1**{E,B}	>20000	IA[c]	1510
2	**1**{E,PE}	IA	IA	1730
3	**2**{E,B,E}	IA	IA	201
4	**2**{E,B,P}	IA	IA	6.01
5	**2**{E,B,B}	364	IA	51.6
6	**2**{E,B,PE}	3830[b]	>10000	42.2
7	**2**{E,PE,E}	IA	479[b]	>10000
8	**2**{E,PE,P}	IA	IA	180
9	**2**{E,PE,B}	IA	IA	>10000
10	**2**{E,PE,PE}	7160[b]	383[b]	382
11	**2**{E,B,2MeOP}	IA	17.2[b]	421
12	**2**{E,B,3MeOP}	IA	IA	3.9
13	**2**{E,B,4MeOP}	4290[b]	IA	12.6
14	**2**{E,B,4MP}	IA	IA	9.2
15	**2**{E,B,4CF3P}	1710[b]	IA	41.7
16	**2**{E,B,4ClP}	IA	IA	78.7
17	**2**{E,B,4BP}	266[b]	IA	7.8
18	**2**{E,B,34DMeOP}	IA	IA	23.8
19	**2**{E,B,35DMeOP}	IA	IA	3.3
20	**2**{E,B,34MeDOP}	IA	IA	3.8
21	WY14643	669	IA	>10000
22	GW501516	>10000	1.4	>10000
23	Rosiglitazone	>10000	>10000	22

[a] units: nM. [b] IC_{50}. [c] inactive.

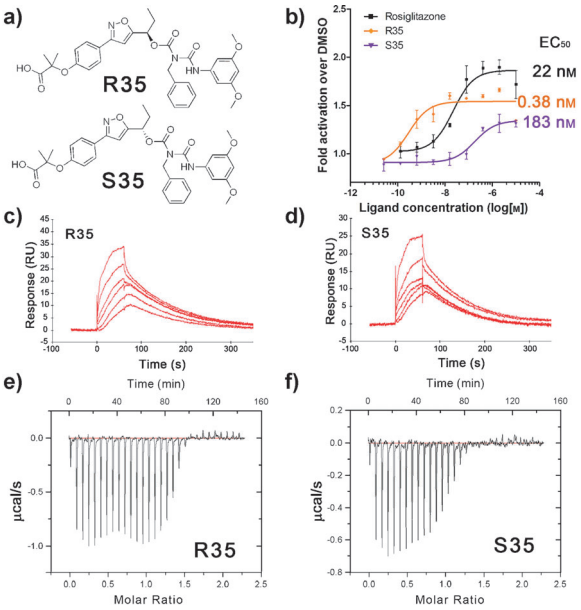

g)

	K_d (µM)			
	ITC		SPR	
Ligand	mouse	human	mouse	human
P29C06	2.1	2.5	1.5	2.2
R35	0.09	0.06	0.17	0.10
S35	0.23	0.49	0.25	0.29
Rosiglitazone	0.32	0.38	0.30	0.28

Figure 3. Identification of **2**{E,B,35DMeOP} as novel ligands of PPARγ. a) Chemical structures of R35 and S35. b) Transactivation profiles of rosiglitazone, R35, and S35 using a PPARγ-derived reporter gene in 293T cells after 24 h treatment ($n=3$). Error bars, s.d. c), d) Sensorgrams from surface plasmon resonance (SPR) assay of R35 (c) and S35 (d) with murine PPARγ ligand-binding domain (mPPARγ-LBD). e), f) Thermograms from isothermal titration calorimetry (ITC) assay of R35 (e) and S35 (f) with mPPARγ-LBD. g) Dissociation constants related to ligand-PPARγ-LBD complex formation determined with ITC or SPR assay. R35, *R*-**2**{E,B,35DMeOP}; S35, *S*-**2**{E,B,35DMeOP}.

assays for all three subtypes of PPAR (PPARα, PPARδ, and PPARγ). Among the initial 8 analogues (entries 3 to 10, Table 1), **2**{E,B,P} exhibited a drastically improved efficacy toward PPARγ from the micromolar to the nanomolar range (1.5 µM to 6.0 nM in EC_{50}) by the simple addition of a second isocyanate moiety to **1**{E,B}. We further diversified the phenyl moiety of **2**{E,B,P} at the R^3 position with various substituents (entries 11 to 20, Table 1) and identified **2**{E,B,35DMeOP} as the best candidate with excellent efficacy (3.3 nM in EC_{50}) and very high selectivity toward PPARγ (entry 19, Table 1).

Prior to the in-depth biological evaluation of this compound, we wanted to address the issue regarding the stereocenter adjacent to the isoxazole ring. To this end, we synthesized two enantiomers of the most active compound, **2**{E,B,35DMeOP} (Figure 3a; Supporting Information, Scheme S2). Interestingly, each enantiomer exhibited different activity in the PPARγ transactivation assay, with the *R* enantiomer (R35) being more potent than its *S* counterpart (S35; Figure 3b). Moreover, the EC_{50} of R35 for PPARγ transactivation was in the sub-nanomolar range, whereas that of S35 was 480-times lower, which suggested that the binding of R35 favors the recruitment of co-activators with proper conformational changes of PPARγ.[13] On the basis of two independent biophysical studies using surface plasmon resonance (SPR) spectroscopy and isothermal titration calorimetry (ITC), we confirmed that the binding affinity of R35 and S35 to the ligand binding domain (LBD) of PPARγ was significantly enhanced from that of P29C06 (Figure 3c–g; Supporting Information, Figures S7, S8, Tables S3, S4). These results indicated that the marginal transcriptional activity of P29C06 was due to its moderate binding affinity to the PPARγ LBD. Along with this, R35 with an EC_{50} of 0.38 nM showed a higher binding affinity to PPARγ, compared to S35 and rosiglitazone. Collectively, we postulated the direct correlation of binding affinity with transactivation ability.

However, we also observed that S35 has a comparable binding affinity to that of rosiglitazone, even though S35 is a much less potent agonist than rosiglitazone. Therefore, we suspected the mode of action of S35 to PPARγ might be different from that of rosiglitazone. To test this hypothesis, we systematically compared our novel PPARγ ligands, R35 and S35, for lead triage. First, both R35 and S35 increased glucose uptake to similar levels, which was measured using [^{14}C]-2-deoxy-D-glucose in adipocytes (Figure 4a). We then sought to determine whether R35 and S35 might serve as inhibitors of the Cdk5-mediated phosphorylation of PPARγ,[14] which is an emerging mode of action for the development of novel antidiabetic agents without the side effects of rosiglitazone, a full PPARγ agonist (Supporting Information, Figure S9).[11a,14,15] Small-molecule ligands that inhibit the phosphorylation of PPARγ at Ser273, such as MRL24, showed an insulin-sensitizing effect in in vitro and in vivo systems by the

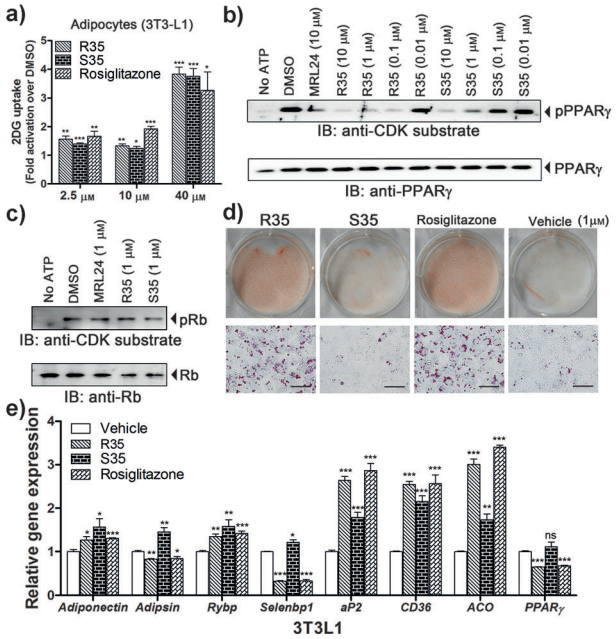

Figure 4. Differential phenotypes upon treatment with R35 and S35. a) Glucose uptake profiles of fully differentiated 3T3L1 cells treated with rosiglitazone, R35, or S35 for 24 h, quantified using [^{14}C]-2-deoxy-D-glucose ($n=4$). b),c) In vitro Cdk5 assay with MRL24, R35, and S35 using PPARγ or Rb as a substrate. IB, immunoblot; NT, not treated; pPPARγ, phosphorylated PPARγ; pRb, phosphorylated Rb. d) Differentiation status of 3T3L1 cells treated with rosiglitazone, R35, or S35 monitored by lipid accumulation with Oil Red O staining; scale bar, 10 μm. e) Relative gene expression patterns by quantitative real-time polymerase chain reaction with RNA extracted from fully differentiated 3TL1 cells treated with rosiglitazone, R35, or S35 (1 μM each) for 24 h ($n=4$). Error bars, s.e.m.; $*P<0.05$, $**P<0.001$, $***P<0.0001$; ns, not significant.

regulation of gene sets related to the phosphorylation of PPARγ.[15] To evaluate their biochemical function, we measured the inhibition of Cdk5-mediated phosphorylation of PPARγ at Ser273 upon treatment with various doses of either R35 or S35 using an in vitro enzymatic assay with purified Cdk5 and PPARγ with MRL24 as a positive control.[14] As shown in Figure 4b, R35 effectively blocked Cdk5-mediated phosphorylation of PPARγ with an IC_{50} between 10 and 100 nM, while S35 showed a slightly lower activity than R35 (IC_{50} between 100 and 1000 nM). Given that neither R35 nor S35 affected Cdk5-mediated phosphorylation of the Rb protein, a known substrate of Cdk5 (Figure 4c),[16] we were confident that the phosphorylation of PPARγ was specifically inhibited by ligand-mediated alteration of the interaction between Cdk5 and PPARγ, rather than an inhibitory effect on general Cdk5 function.

In fact, the full agonism on PPARγ triggers adipogenesis in fibroblasts,[11b,d] which is a major adverse effect of rosiglitazone.[14,15] As shown in Figure 4d, R35 potentiated adipocyte differentiation to a similar level of rosiglitazone, confirmed by the monitoring of cellular lipid accumulation with Oil Red O staining. However, in the case of S35, we observed extremely low levels of lipid accumulation, which was comparable to that of the vehicle control. Finally, we examined the ligand-mediated expression of genes related to fatty acid metabolism, including *aP2*, *CD36*, and *ACO*, which are known to be increased upon treatment with PPARγ agonists.[17] As expected, the treatment of 3T3L1 adipocytes with R35 increased the expression of *aP2*, *CD36*, and *ACO*, whereas S35 exerted only a marginal effect. On the other hand, both R35 and S35 caused increases in the expression of *Adiponectin* and *Rybp*, the genes that are most sensitive to the phosphorylation of PPARγ at Ser273.[15] Most importantly, only S35 increased the expression level of *Adipsin* and *Selenbp1*, whereas R35 and rosiglitazone reduced the expression of these genes (Figure 4e). These secondary biochemical evaluations imply that stereoisomeric differences in R35 and S35 may have different effects on gene expression, adipogenesis, and PPARγ phosphorylation. R35 behaves as a conventional PPARγ agonist while S35 deviated from agonism with high correlation in the phosphorylation inhibitory event unlike conventional PPARγ agonists. Therefore, S35 may serve as a key structural clue for the development of new PPARγ-related therapeutic agents to treat glucose homeostasis-related diseases without side effects.

In summary, we demonstrated the hit-to-lead optimization of new small-molecule enhancers of cellular glucose uptake, discovered from image-based phenotypic screening in myotubes. Our initial hit compounds were subjected to FITGE-guided target identification, which revealed PPARγ as the target protein in adipocytes. The subsequent rational optimization of the initial hits generated a lead compound with high potency (4000-fold enhancement from initial hit). Secondary biophysical and biochemical studies revealed the stereoisomeric difference in our optimized PPARγ ligands (R35 and S35) dictating their transcriptional activity, binding affinity, and inhibitory activity toward Cdk5-mediated phosphorylation of PPARγ at Ser273. It turned out that S35 is a PPARγ phosphorylation inhibitor with promising glucose uptake potential, while R35 is a highly potent conventional PPARγ agonist; therefore, our PPARγ ligands, especially S35, can be utilized for the development of new anti-diabetic agents without side effects. In light of high demands for a new class of therapeutic agents, the novel scaffolds identified from unbiased phenotypic screening and target identification can be a powerful resource for the development of first-in-class drugs.

Received: December 7, 2013
Revised: February 21, 2014
Published online: April 1, 2014

Keywords: drug discovery · glucose uptake · phenotypic screening · PPARγ · target identification

[1] a) E. Cohen, A. Dillin, *Nat. Rev. Neurosci.* **2008**, *9*, 759–767; b) D. M. Nathan, J. B. Buse, M. B. Davidson, E. Ferrannini, R. R. Holman, R. Sherwin, B. Zinman, A. American Diabetes, D. European Association for Study of, *Diabetes Care* **2009**, *32*, 193–203; c) C. F. Semenkovich, *J. Clin. Invest.* **2006**, *116*, 1813–1822.

[2] M. Kars, L. Yang, M. F. Gregor, B. S. Mohammed, T. A. Pietka, B. N. Finck, B. W. Patterson, J. D. Horton, B. Mittendorfer, G. S. Hotamisligil, S. Klein, *Diabetes* **2010**, *59*, 1899 – 1905.
[3] A. Jo, J. Park, S. B. Park, *Chem. Commun.* **2013**, *49*, 5138 – 5140.
[4] a) H. Y. Lee, J. J. Lee, J. Park, S. B. Park, *Chem. Eur. J.* **2011**, *17*, 143 – 150; b) J. Park, H. Y. Lee, M. H. Cho, S. B. Park, *Angew. Chem.* **2007**, *119*, 2064 – 2068; *Angew. Chem. Int. Ed.* **2007**, *46*, 2018 – 2022; c) Y. S. Tian, H. Y. Lee, C. S. Lim, J. Park, H. M. Kim, Y. N. Shin, E. S. Kim, H. J. Jeon, S. B. Park, B. R. Cho, *Angew. Chem.* **2009**, *121*, 8171 – 8175; *Angew. Chem. Int. Ed.* **2009**, *48*, 8027 – 8031.
[5] J. Park, S. Oh, S. B. Park, *Angew. Chem.* **2012**, *124*, 5543 – 5547; *Angew. Chem. Int. Ed.* **2012**, *51*, 5447 – 5451.
[6] S. Oh, S. B. Park, *Chem. Commun.* **2011**, *47*, 12754 – 12761.
[7] S. Oh, S. J. Kim, J. H. Hwang, H. Y. Lee, M. J. Ryu, J. Park, S. J. Kim, Y. S. Jo, Y. K. Kim, C. H. Lee, K. R. Kweon, M. Shong, S. B. Park, *J. Med. Chem.* **2010**, *53*, 7405 – 7413.
[8] M. W. Rajala, P. E. Scherer, *Endocrinology* **2003**, *144*, 3765 – 3773.
[9] J. V. Staros, *Trends Biochem. Sci.* **1980**, *5*, 320 – 322.
[10] K. K. Ryan, B. Li, B. E. Grayson, E. K. Matter, S. C. Woods, R. J. Seeley, *Nat. Med.* **2011**, *17*, 623 – 626.
[11] a) M. Ahmadian, J. M. Suh, N. Hah, C. Liddle, A. R. Atkins, M. Downes, R. M. Evans, *Nat. Med.* **2013**, *19*, 557 – 566; b) T. Albrektsen, K. S. Frederiksen, W. E. Holmes, E. Boel, K. Taylor, J. Fleckner, *Diabetes* **2002**, *51*, 1042 – 1051; c) R. K. Semple, V. K. Chatterjee, S. O'Rahilly, *J. Clin. Invest.* **2006**, *116*, 581 – 589; d) P. Tontonoz, E. Hu, B. M. Spiegelman, *Cell* **1994**, *79*, 1147 – 1156.
[12] R. T. Nolte, G. B. Wisely, S. Westin, J. E. Cobb, M. H. Lambert, R. Kurokawa, M. G. Rosenfeld, T. M. Willson, C. K. Glass, M. V. Milburn, *Nature* **1998**, *395*, 137 – 143.
[13] B. C. Kallenberger, J. D. Love, V. K. Chatterjee, J. W. Schwabe, *Nat. Struct. Biol.* **2003**, *10*, 136 – 140.
[14] J. H. Choi, A. S. Banks, J. L. Estall, S. Kajimura, P. Bostrom, D. Laznik, J. L. Ruas, M. J. Chalmers, T. M. Kamenecka, M. Blüher, P. R. Griffin, B. M. Spiegelman, *Nature* **2010**, *466*, 451 – 456.
[15] J. H. Choi, A. S. Banks, T. M. Kamenecka, S. A. Busby, M. J. Chalmers, N. Kumar, D. S. Kuruvilla, Y. Shin, Y. He, J. B. Bruning, D. P. Marciano, M. D. Cameron, D. Laznik, M. J. Jurczak, S. C. Schurer, D. Vidović, G. I. Shulman, B. M. Spiegelman, P. R. Griffin, *Nature* **2011**, *477*, 477 – 481.
[16] X. Graña, A. De Luca, N. Sang, Y. Fu, P. P. Claudio, J. Rosenblatt, D. O. Morgan, A. Giordano, *Proc. Natl. Acad. Sci. USA* **1994**, *91*, 3834 – 3838.
[17] M. Schupp, M. Clemenz, R. Gineste, H. Witt, J. Janke, S. Helleboid, N. Hennuyer, P. Ruiz, T. Unger, B. Staels, U. Kintscher, *Diabetes* **2005**, *54*, 3442 – 3452.

